

Corrosion protection of AZ91 magnesium alloy in cooling systems

D. SEIFZADEH, H. BASHARNAVAZ

Physical Chemistry Research Laboratory, Applied Chemistry Department, Faculty of Science,
University of Mohaghegh Ardabili, Ardabil, Iran

Received 29 September 2012; accepted 28 January 2013

Abstract: The effect of a salicylic Schiff base compound (Salcn) on the corrosion of AZ91 alloy in 30% ethylene glycol aqueous solution (30% EG/W) was investigated by electrochemical methods. Scanning electron microscope was used to observe the alloy surface in corrosive solution before and after the addition of inhibitor. There was no significant corrosion inhibition at the room temperature but high inhibition efficiencies were obtained at elevated temperatures due to the formation of chemisorbed inhibitor monolayer. As the inhibitor concentration increased, the inhibition efficiency increased probably due to more inhibitor adsorption on the alloy surface.

Key words: AZ91 magnesium alloy; ethylene glycol aqueous solution; corrosion; inhibition

1 Introduction

Magnesium alloys are increasingly used in aerospace and automotive industries owing to their ultra-lightness (their density is two thirds that of aluminum and one fourth that of iron) and high specific strength. These alloys appear to be promising alternatives to aluminum and steel alloys used in different applications [1–3]. However, poor corrosion resistance of magnesium alloys limits their widespread application. For example, in cooling system of the magnesium engine, corrosion is always a major concern [4,5]. The main composition of a conventional coolant consists of 30%–70% (by volume) ethylene glycols and some corrosion inhibitors. The inhibitors normally include molybdate, phosphate, borate, nitrate, nitrite, tolyltriazole, benzoate and silicate which can protect traditional engine materials, such as cast iron, aluminum, copper, steel and lead–tin solder [6]. However, magnesium alloys are new materials in engine applications and it is still unclear whether existing inhibitors can be used for its corrosion protection in ethylene glycol coolant solution.

Currently, there is limited information about corrosion inhibition of magnesium or its alloys in ethylene glycol solutions. Lactobionic acid derivatives [7] and aliphatic or aromatic carboxylates [5], besides

some inorganic salts, have been tested in ethylene glycol/water solutions as magnesium corrosion inhibitors.

Due to the presence of —C=N group in the Schiff base molecules, they are likely to be good corrosion inhibitors [8]. Schiff base compounds have extensively been investigated as effective corrosion inhibitors for steel [8–10], aluminum [11–13] and copper [14] in different corrosive media.

The aim of this work is to investigate the inhibition effect of a Salicylic Schiff base compound (Salcn) on AZ91 magnesium alloys corrosion in ethylene glycol coolant systems. The presented results may form a base for development of new organic inhibitor packages for magnesium alloys engine blocks.

2 Experimental

2.1 Materials

Chemical structure of the studied Schiff base compound (Salcn) is shown in Fig. 1. Salcn was synthesized by the condensation reaction between 1,2-cyclohexandiamin and salicylaldehyde. Firstly, 50 mL ethanol solution containing 4.0 mmol of salicylaldehyde was added drop wise to 10 mL ethanol solution containing 2.0 mmol of 1,2-cyclohexandiamin under continuous stirring. Precipitation of Salcn as brilliant yellow flakes in the solution started almost

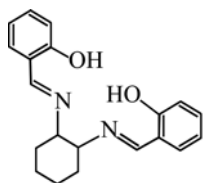


Fig. 1 Chemical structure of studied Schiff base compound

immediately. This mixture was then stirred for 1 h in order to promote the rate of chemical reaction. Then, the solid was filtered and washed with cold ethanol. Finally, the obtained compound was recrystallized in ethanol and dried at room temperature. All chemicals were purchased from Merck.

The samples for this study were commercial cast AZ91 alloy. The AZ91 magnesium alloy has a nominal composition as Al 9% (mass fraction), Zn 1% (mass fraction) and Mg balance. Alloy samples with dimensions of 1 cm × 1 cm × 1 cm were mounted in polyester in such a way that only 1 cm² of their surfaces was in contact with corrosive solution. The AZ91 samples were abraded with 400–800 and 1500 emery papers and then washed with tap water, and degreased with ethanol before being immediately immersed in the corrosive solution. The corrosive solution was 30% (by volume) ethylene glycol in water (30% EG/W). Two different concentrations (0.001 and 0.0015 mol/L) of Salcn were examined for their corrosion inhibition effect. The concentration of 0.0015 mol/L is the highest level of solubility of Salcn in 30% EG/W at room temperature. The volume of test solution for each experiment was 200 mL and all experiments were carried out under ambient pressure. No solution deaeration was conducted during tests in this study.

2.2 Methods

2.2.1 Electrochemical methods

A three-electrode cell, consisting of alloy sample as working electrode, platinum sheet as a counter electrode (CE), and a saturated Ag/AgCl electrode as reference electrode, was used in electrochemical measurements. Electrochemical tests were carried out using a μautolab3 Potentiostat-Galvanostat. Nova (version 1.6) software was used for data recording. For polarization measurements, the potential was scanned with a scan rate of 2 mV/s in the cathodic to anodic direction, so that the maximum over voltage was around 200 mV. EIS measurements were performed in the frequency range of 1 MHz–0.4 Hz, at the open circuit potential, by applying 5 mV sine wave AC voltage.

2.2.2 SEM observation

Surface morphology of the AZ91 alloy specimens was observed by SEM (LEO, VP 1430) instrument

before and after the immersion in the inhibited and blank coolant solutions.

3 Results and discussion

3.1 Potentiodynamic polarization

The potentiodynamic polarization curves of AZ91 in the 30% EG/W solution with two different concentrations of the Salcn (0.001 and 0.0015 mol/L) at 25, 50 and 75 °C are displayed in Fig. 2. Activation-

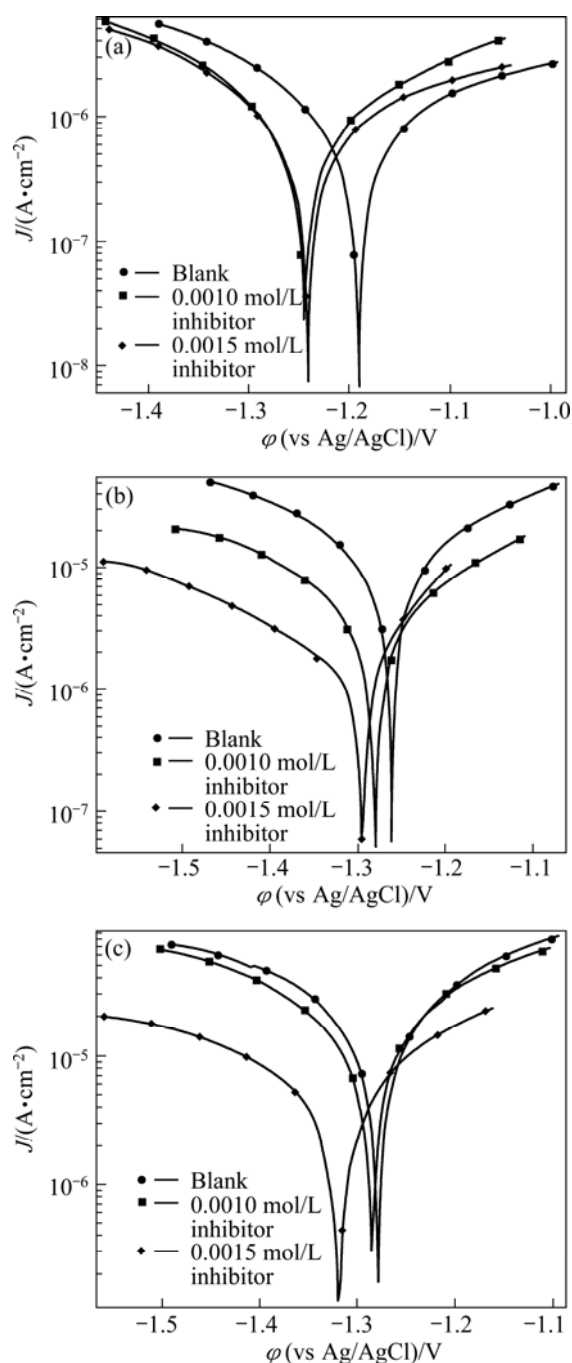


Fig. 2 Polarization curves for AZ91 alloy in blank 30% EG/W solution and solution containing two various concentrations of Salcn at different temperatures: (a) 25 °C; (b) 50 °C; (c) 75 °C

controlled anodic and cathodic corrosion reactions can be observed either in the absence or presence of the Salcn at all temperatures. The anodic process is the dissolution of the main alloying elements (Mg, Al and Zn) while the cathodic reaction is the reduction of water which produces hydrogen bubbles. Both the anodic and cathodic currents decrease after the addition of the Salcn Schiff base to the corrosive solution at 50 °C and 75 °C while there is no significant inhibition effect at 25 °C. These results suggest that the addition of the Salcn Schiff base reduces the anodic dissolution and also retards the hydrogen evolution reaction at elevated temperatures. The corrosion inhibition effect is more evident in the cathodic branch of polarization curves. The values of corrosion potential (φ_{corr}) in the absence and presence of the Salcn at two different concentrations are given in Table 1. It is clearly seen that the corrosion potential values shift to the negative direction after the addition of the Salcn. This fact shows that the Salcn mainly acts via the adsorption on the cathodic corrosion sites. Generally, if the displacement in φ_{corr} in the presence of inhibitor is bigger than 85 mV, the inhibitor can be classified as a cathodic or anodic type; if the displacement is less than 85 mV, the inhibitor can be considered mixed type [5]. In this case, the maximum displacement in φ_{corr} value is lower than 85 mV towards cathodic direction, which indicates that the Salcn acts as a mixed type inhibitor.

Other corrosion parameters, such as cathodic and anodic Tafel slopes (B_c and B_a), polarization resistance (R_p) and corrosion current (J_{corr}), are also obtained from the polarization curves (Table 1). At the elevated temperatures, the addition of Schiff base increases the polarization resistance of AZ91 and this fact leads to a reduction in corrosion current. This means that the used compound acts as an effective inhibitor for AZ91 in the 30% EG/W solution at elevated temperatures. Corrosion inhibition efficiencies (IE) are calculated from the following equation [15]:

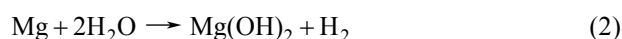
$$IE = \left(\frac{R_{\text{inh}} - R_{\text{Blank}}}{R_{\text{inh}}} \right) \times 100\% \quad (1)$$

where R_{Blank} and R_{inh} are polarization resistance of the uninhibited and inhibited corrosive solutions, respectively. The values of corrosion inhibition efficiencies are also listed in Table 1. As the inhibitor concentration increases, the inhibition efficiency increases at all temperatures studied, probably because of more inhibitor adsorption on the alloy surface.

Analysis of the temperature dependence of inhibition efficiency gives some useful information about the mechanism of inhibitor adsorption. A decrease in inhibition efficiency with rise in temperature is frequently interpreted as being suggestive of multilayer physical adsorption mechanism, while the reverse effect, corresponding to an increase in inhibition efficiency with rise in temperature, suggests the formation of a chemisorbed monolayer [16–19].

It is clear from Table 1 that there is no significant inhibition efficiency at 25 °C and only the low level of corrosion inhibition can be observed in the presence of 0.0015 mol/L Salcn. Different results can be observed at elevated temperatures where the Salcn effectively inhibits the corrosion process. Therefore, it seems that a higher temperature is favorable for the adsorption of inhibitors on the alloy surface. These results indicate that the studied inhibitor acts on the alloy surface via chemical adsorption.

The overall corrosion reaction of magnesium in aqueous solution is [20]



Therefore, in water containing solution, the surface of a Mg alloy is likely covered by a layer of $\text{Mg}(\text{OH})_2$ film, which has many defects or pores and is not completely protective. The adsorption of Salcn on the metal surface through the pores should be responsible for

Table 1 Polarization parameters for AZ91 alloy samples in 30% EG/W in the absence and presence of Salcn at different temperatures

Temperature/ °C	Salcn concentration/ (mol·L ⁻¹)	φ_{corr} (vs Ag/AgCl)/ V	R_p / (kΩ·cm ²)	B_a / (mV·dec ⁻¹)	B_c / (mV·dec ⁻¹)	J_{corr} / (μA·cm ⁻²)	IE/%
25	Blank	-1.190	68.8	109	140	0.39	–
	0.0010	-1.246	62.7	117	135	0.43	-9.73
	0.0015	-1.241	74.0	107	145	0.36	7.03
50	Blank	-1.261	4.7	94	163	5.45	–
	0.0010	-1.280	13.8	150	149	2.35	65.94
	0.0015	-1.297	24.8	216	90	1.11	81.05
75	Blank	-1.279	3.2	166	150	10.69	–
	0.0010	-1.287	3.9	144	170	8.75	17.95
	0.0015	-1.320	11.1	184	142	3.15	71.17

the improved polarization resistance. In other words, the adsorption of the Schiff base molecule on the film-free area makes the surface film denser or less defective and significantly decreases the dissolution of Mg through the pore [20]. Salcn contains oxygen and nitrogen hetero atoms, C=N groups and also aromatic rings and therefore can provide electrons to unoccupied orbital of the alloying metals to form covalent bonds. Also the chemical adsorption may be possible via the condensation reaction between the OH groups of the Schiff base molecule and the magnesium hydroxide film.

Inhibition efficiency decreases with increasing temperature from 50 °C to 75 °C especially at low concentration of inhibitor. This is due to high corrosion rate and also may be related with high rate of hydrogen evolution which can facilitate desorption of the inhibitor molecules [20]. However, the Salcn Schiff base keeps the high level of corrosion inhibition at 0.0015 mol/L concentration even at the highest elevated temperature. It should be stressed that a high inhibition efficiency at a high temperature is a critical property of an inhibitor in the engine coolant application. Not many inhibitors can maintain high inhibition efficiency at an elevated temperature.

3.2 EIS analysis

Electrochemical impedance spectroscopy was also employed as a powerful complementary technique to study the corrosion inhibition effect of the Salcn Schiff base in 30% EG/W. The impedance response (Nyquist, modulus and phase Bode plots) of AZ91 in the absence and presence of the Salcn at different temperatures are shown in Figs. 3–5.

In the Nyquist plots, there are two well defined capacitive loops at the high and low frequency ranges, respectively. The first loop at the higher frequencies could be assigned to the capacitance and resistance of the porous film on the AZ91 alloy surface, while the second loop at low frequencies should be related to the electrical double layer between the metal and the corrosive solution. In fact, the second loop is related to the charge transfer process at the boundary between the metal surface and corrosive solution through the pores in the film. In order to obtain quantitative results, the impedance spectra were fitted using a convenient equivalent circuit model (Fig. 6). In this model, R_s , R_{ct} and R_{pore} characterize the solution resistance, the charge transfer resistance and the pores resistance, respectively. The first capacitive element (C_f) is related to the porous film capacitance, while the other time constant is representative of the electrical double layer capacitance (CPE_{dl}). The constant phase element (CPE) is used instead of ideal capacitive component to account for non-ideal behavior of double layer capacitor due to

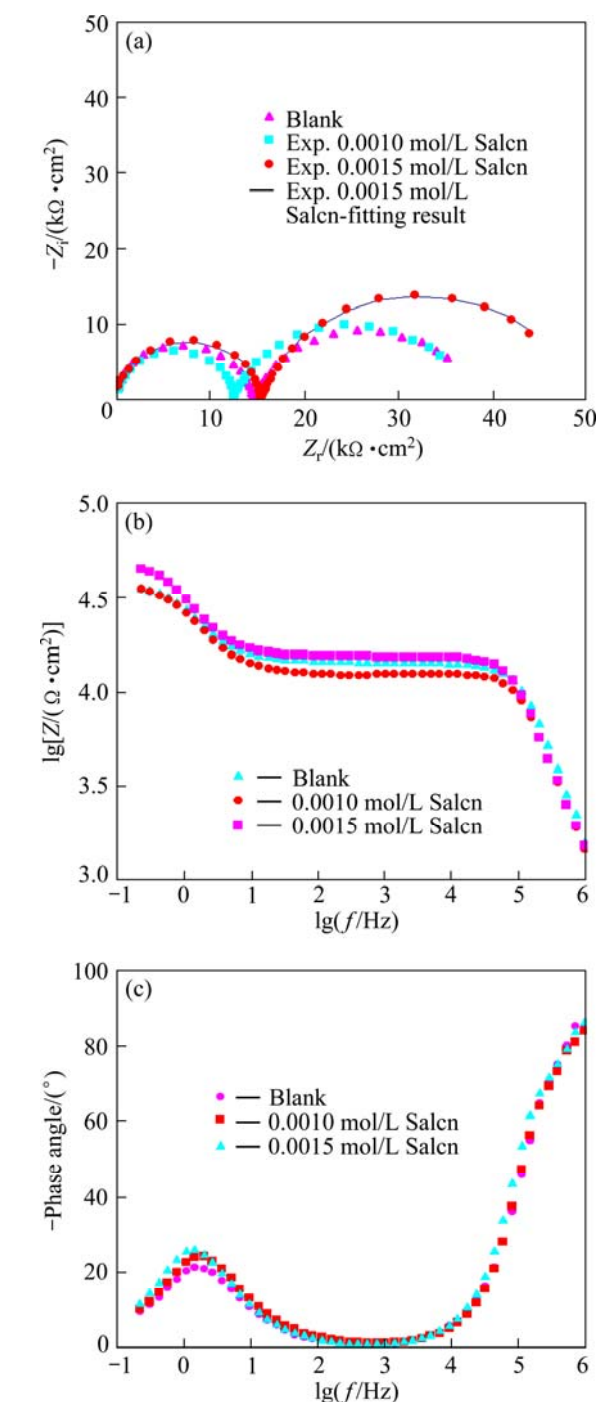


Fig. 3 Nyquist (a), modulus (b) and phase Bode (c) plots of AZ91 in 30% EG/W in the absence and presence of Salcn at 25 °C

surface inhomogeneity, roughness and adsorption effects [5,8,9,21]. The impedance of CPE is given in Ref. [22] as

$$Z_{CPE} = \frac{1}{Q} (j\omega)^{-n} \quad (3)$$

where Q is the CPE constant; ω is the angular frequency; $j = \sqrt{-1}$ is the imaginary number; n is a

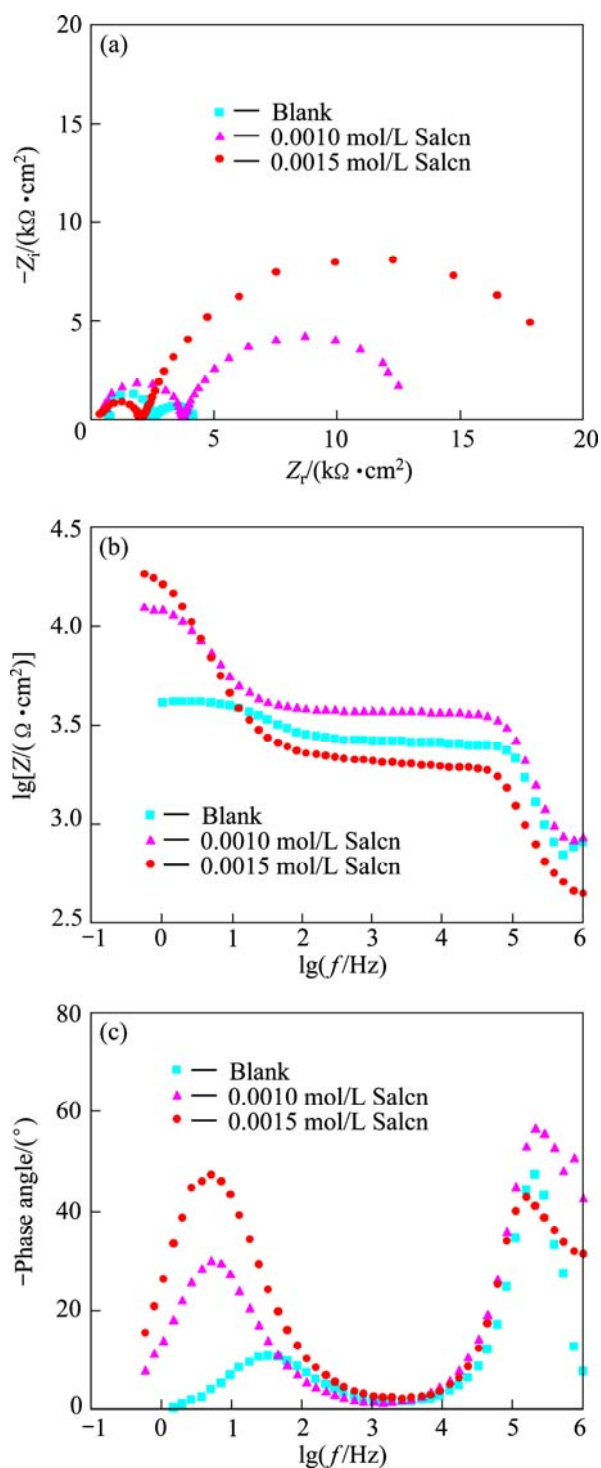


Fig. 4 Nyquist (a), modulus (b) and phase Bode (c) plots of AZ91 in 30% EG/W in the absence and presence of Salcn at 50 °C

CPE exponent which can be used as a gauge of the heterogeneity or roughness of the surface [23]. Depending on the value of n , CPE can represent resistance ($n=0$, $Q=R$), capacitance ($n=1$, $Q=C$), inductance ($n=-1$, $Q=L$) or Warburg impedance ($n=0.5$, $Q=W$) [24]. The capacitance values of electrical double layer were calculated according to the following equation [25]:

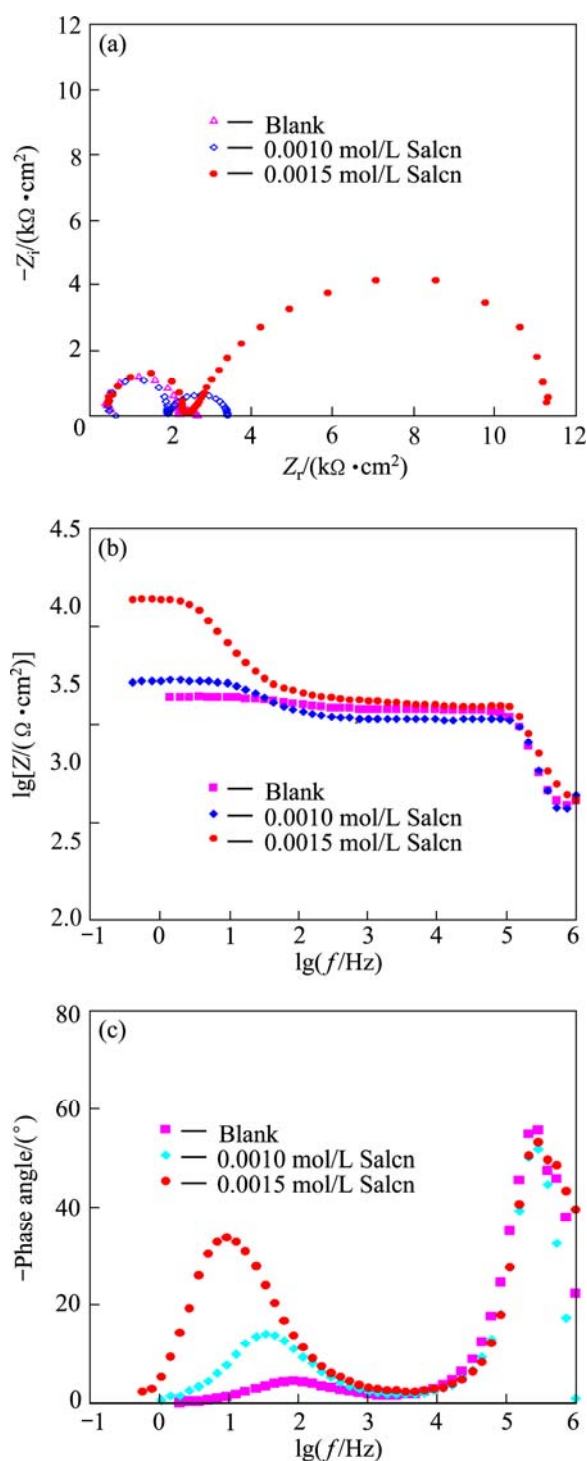


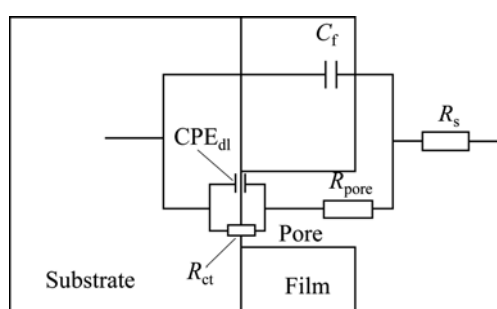
Fig. 5 Nyquist (a), modulus (b) and phase Bode (c) plots of AZ91 in 30% EG/W in the absence and presence of Salcn at 75 °C

$$C = (QR_{ct}^{1-n})^{\frac{1}{n}} \quad (4)$$

The EIS data were fitted by Zview2 software using the described electrical model. The quantitative impedance parameters are collected in Table 2. The total resistance of the electrode surface ($R_{total}=R_t+R_{pore}$) was used to calculate the inhibition efficiencies of the Salcn

Table 2 Impedance parameters for AZ91 alloy samples in 30% EG/W in the absence and presence of Salcn at different temperatures

Temperature/ °C	Salcn concentration/ (mol·L ⁻¹)	C_f / (nF·cm ²)	R_{pore} / (kΩ·cm ²)	Q_{dl} / (μs ⁿ ·Ω ⁻¹ ·cm ⁻²)	n_{dl}	C_{dl} / (μF·cm ²)	R_{ct} / (kΩ·cm ²)
25	Blank	0.099	14.58	9.450	0.831	6.992	24.11
	0.0010	0.116	12.48	8.607	0.847	6.525	25.14
	0.0015	0.115	15.36	7.820	0.861	6.311	34.07
50	Blank	0.719	1.81	11.353	0.758	3.287	1.82
	0.0010	0.464	3.44	7.627	0.904	5.781	9.59
	0.0015	1.144	1.68	7.263	0.876	5.501	19.21
75	Blank	0.650	1.75	0.194	0.74102	3.879	0.51
	0.0010	0.720	1.37	7.536	0.8561	3.579	1.58
	0.0015	0.463	2.17	5.074	0.882	3.379	9.43

**Fig. 6** Equivalent circuit used for fitting of EIS data

Schiff base at different concentrations based on the following equation:

$$IE = \left(\frac{R_{\text{total}} - R_{\text{total}}^0}{R_{\text{total}}} \right) \times 100\% \quad (5)$$

where R_{total}^0 and R_{total} are the total resistances of AZ91 alloy in the blank and inhibited solutions, respectively. The calculated values are given in Table 3. The inhibition efficiencies calculated from EIS results show the same trend as those obtained from potentiodynamic polarization measurements. It is clear from Table 2 that the R_t values increase with the increasing concentration

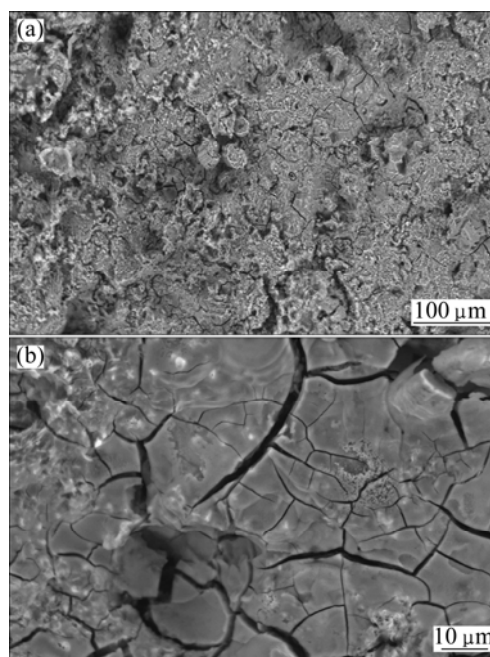
Table 3 Calculated IE values by Eq. (5)

Temperature/ °C	Salcn concentration/ (mol·L ⁻¹)	R_{total} / (kΩ·cm ²)	IE/%
25	Blank	38.69	–
	0.0010	37.62	–2.84
	0.0015	49.43	21.73
50	Blank	3.63	–
	0.0010	13.03	72.14
	0.0015	20.89	82.62
75	Blank	2.26	–
	0.0010	2.95	23.39
	0.0015	11.60	80.52

of the inhibitors. On the other hand, the values of CPE_{dl} decrease with an increase in the inhibitors concentration thus with inhibition efficiencies. This situation is the result of an increase in the surface coverage by the inhibitor, which leads to an increase in the inhibition efficiency. The decrease in the CPE_{dl} , which can result from a decrease in local dielectric constant and/or an increase in the thickness of the electrical double layer, suggests that the Salcn molecule acts at the metal/solution interface by adsorption [8,9,26].

3.3 SEM observation

The SEM images of AZ91 samples in the blank corrosive solution and in the solution containing 0.0015 mol/L Salcn after 2 d immersion at 50 °C are shown in Figs. 7 and 8, respectively. The related images are shown

**Fig. 7** SEM images of AZ91 alloy sample in blank corrosive solution after 2 d immersion at 50 °C at low (a) and high (b) magnifications

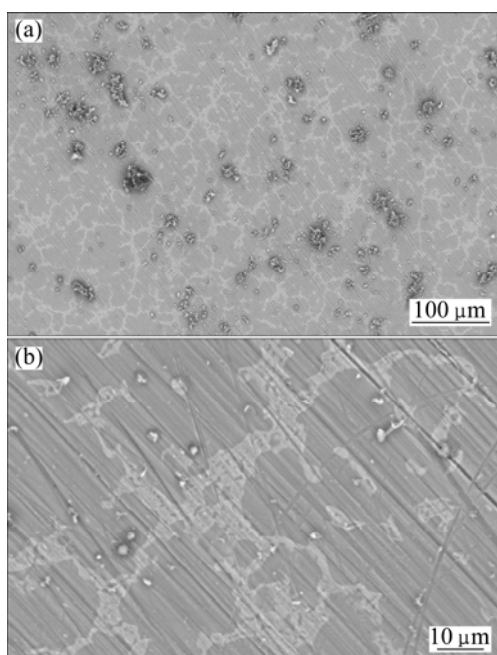


Fig. 8 SEM images of AZ91 alloy sample in test solution containing 0.0015 mol/L Salcn after 2 d immersion at 50 °C at low (a) and high (b) magnifications

in two different magnifications. It can be seen from Figs. 7(a) and (b) that the alloy surface is strongly damaged in the absence of inhibitor. In the case of inhibited samples, it can be seen that the alloy surface is uniform without obvious defects. The related images (Figs. 8(a) and (b)) show that the surface of the alloy is absolutely free from any pits and cracks so that the polishing scratches are also visible, indicating the very low corrosion of the sample during the immersion period.

4 Conclusions

1) Salcn acts as effective corrosion inhibitor for AZ91 magnesium in 30% EG/W solution.

2) Corrosion inhibition efficiencies of the Salcn Schiff base increase with increasing concentration due to more inhibitor adsorption on the alloy surface, and the results obtained from polarization and EIS methods match one another.

3) The inhibition efficiency of the Salcn increases with increasing temperature from 25 °C to 50 °C, indicating the chemisorption of the inhibitor molecules on alloy surface.

4) As the inhibitor concentration increases, the values of R_{ct} increase and the values of CPE_{dl} decrease.

Acknowledgment

The authors wish to thank the Research Council of the University of Mohaghegh Ardabili for its financial support of this study.

References

- [1] HU Jun-ying, HUANG Dao-bing, SONG Guang-ling, GUO Xing-peng. The synergistic inhibition effect of organic silicate and inorganic Zn salt on corrosion of Mg–10Gd–3Y magnesium alloy [J]. *Corrosion Science*, 2011, 53: 4093–4101.
- [2] ZHANG Tao, LIU Xiao-lan, SHAO Ya-wei, MENG Guo-zhe, WANG Fu-hui. Electrochemical noise analysis on the pit corrosion susceptibility of Mg–10Gd–2Y–0.5Zr, AZ91D alloy and pure magnesium using stochastic model [J]. *Corrosion Science*, 2008, 50: 3500–3507.
- [3] SONG G L, BOWLES A L, StJOHN D H. Corrosion resistance of aged die cast magnesium alloy AZ91D [J]. *Materials Science and Engineering A*, 2004, 366: 74–86.
- [4] MONTEMOR M F, SIMOES A M, CARMEZIM M J. Characterization of rare-earth conversion films formed on the AZ31 magnesium alloy and its relation with corrosion protection [J]. *Applied Surface Science*, 2007, 253: 6922–6931.
- [5] TORRESS V V, AMADO R S, de SÁ C F, FERNANDEZ T L, da SILVA RIEHI C A, TORRES A G, D'ELIA E. Inhibitory action of aqueous coffee ground extracts on the corrosion of carbon steel in HCl solution [J]. *Corrosion Science*, 2011, 53: 2385–2392.
- [6] SONG G L, StJOHN D H. Corrosion behaviour of magnesium in ethylene glycol [J]. *Corrosion Science*, 2004, 46: 1381–1399.
- [7] SLAVCHEVA E, PETKOVA G, ANDREEV P. Inhibition of corrosion of AZ91 magnesium alloy in ethylene glycol solution in presence of chloride anions [J]. *Materials Corrosion*, 2005, 56: 83–87.
- [8] SORKHABI H A, SHAABANI B, SEIFZADEH D. Corrosion inhibition of mild steel by some Schiff base compounds in hydrochloric acid [J]. *Applied Surface Science*, 2005, 239: 154–164.
- [9] SORKHABI H A, SHAABANI B, SEIFZADEH D. Effect of some pyrimidinic Schiff bases on the corrosion of mild steel in hydrochloric acid solution [J]. *Electrochimica Acta*, 2005, 50: 3446–3452.
- [10] SOLMAZ R, ALTUNBAS E, KARDAS G. Adsorption and corrosion inhibition effect of 2-(5-mercapto-1,3,4-thiadiazol-2-ylimino) methyl phenol Schiff base on mild steel [J]. *Materials Chemistry and Physics*, 2011, 125: 796–801.
- [11] SORKHABI H A, SHAABANI B, ALIGHOLIPOUR B, SEIFZADEH D. The effect of some Schiff bases on the corrosion of aluminum in hydrochloric acid solution [J]. *Applied Surface Science*, 2006, 252: 4039–4047.
- [12] NEGM N A, ZAKI M F. Corrosion inhibition efficiency of nonionic Schiff base amphiphiles of *p*-aminobenzoic acid for aluminum in 4 N HCl [J]. *Colloids and Surfaces A*, 2008, 322: 97–102.
- [13] YURT A, ULUTAS S, DAL H. Electrochemical and theoretical investigation on the corrosion of aluminium in acidic solution containing some Schiff bases [J]. *Applied Surface Science*, 2006, 253: 919–925.
- [14] BEHPOUR M, GHOREISHI S M, NIASARI M S, EBRAHIMI B. Evaluating two new synthesized S–N Schiff bases on the corrosion of copper in 15% hydrochloric acid [J]. *Materials Chemistry and Physics*, 2008, 107: 153–157.
- [15] SORKHABI H A, SEIFZADEH D. Analysis of raw and trend removed EN data in time domain to evaluate corrosion inhibition effects of new Fuchsin dye on steel corrosion and comparison of results with EIS [J]. *Journal of Applied Electrochemistry*, 2008, 38: 1545–1552.
- [16] OGUZIE E E, OKOLUE B N, OGUKWE C E, UNAEGBU C. Corrosion inhibition and adsorption behaviour of bismark brown dye on aluminium in sodium hydroxide solution [J]. *Material Letters*, 2006, 60: 3376–3378.

- [17] OGUZIE E E, OKOLUE B N, EBENSO E E, ONUOHA G N, ONUCHUKWU A I. Evaluation of the inhibitory effect of methylene blue dye on the corrosion of aluminium in hydrochloric acid [J]. *Materials Chemistry and Physics*, 2004, 87: 394–401.
- [18] MARTINEZ S, STERN I. Inhibitory mechanism of low-carbon steel corrosion by mimosa tannin in sulphuric acid solutions [J]. *Journal of Applied Electrochemistry*, 2001, 31: 973–978.
- [19] POPOVA A, SOKOLOVA E, RAICHEVA S, CHRISTOV M. AC and DC study of the temperature effect on mild steel corrosion in acid media in the presence of benzimidazole derivatives [J]. *Corrosion Science*, 2003, 45: 33–58.
- [20] HUANG Dao-bing, HU Jun-ying, SONG Guang-ling, GUO Xing-peng. Inhibition effect of inorganic and organic inhibitors on the corrosion of Mg–10Gd–3Y–0.5Zr alloy in an ethylene glycol solution at ambient and elevated temperatures [J]. *Electrochimica Acta*, 2011, 56: 10166–10178.
- [21] SORKHABI H A, SEIFZADEH D, HOSSEINI M G. EN, EIS and polarization studies to evaluate the inhibition effect of 3H-phenothiazin-3-one, 7-dimethylamin on mild steel corrosion in 1 M HCl solution [J]. *Corrosion Science*, 2008, 50: 3363–3370.
- [22] BENTISS F, JAMA C, MERNARI B, EI ATTARI H, EI KADI L, LEBRINI M, TRAISNEL M, LAGRENEE M. Corrosion control of mild steel using 3,5-bis(4-methoxyphenyl)-4-amino-1,2,4-triazole in normal hydrochloric acid medium [J]. *Corrosion Science*, 2009, 51: 1628–1635.
- [23] LOPEZ D A, SIMISON S N, de SANCHEZ S R. The influence of steel microstructure on CO₂ corrosion. EIS studies on the inhibition efficiency of benzimidazole [J]. *Electrochimica Acta*, 2003, 48: 845–854.
- [24] MORAD M S. An electrochemical study on the inhibiting action of some organic phosphonium compounds on the corrosion of mild steel in aerated acid solutions [J]. *Corrosion Science*, 2000, 42: 1307–1326.
- [25] MAHDAVIAN M, NADERI R. Corrosion inhibition of mild steel in sodium chloride solution by some zinc complexes [J]. *Corrosion Science*, 2011, 53: 1194–1200.
- [26] BENABDELLAH M, TOUZANI R, AOUNITI A, DAFALI A, EL KADIRI S, HAMMOUTI B, BENKADDOUR M. Inhibitive action of some bipyrazolic compounds on the corrosion of steel in 1 M HCl: Part I: Electrochemical study [J]. *Materials Chemistry and Physics*, 2007, 105: 373–379.

AZ91 镁合金在冷却系统中的耐腐蚀性

D. SEIFZADEH, H. BASHARNAVAZ

Physical Chemistry Research Laboratory, Applied Chemistry Department, Faculty of Science,
University of Mohaghegh Ardabili, Ardabil, Iran

摘要: 运用电化学方法研究一种水杨酸 Schiff 碱化合物(Salcn)对 AZ91 镁合金在 30%乙二醇水溶液(30% EG/W)中的腐蚀行为的抑制作用。用扫描电镜观察合金在 30%乙二醇水溶液(30% EG/W)中的腐蚀前、后的形貌。在室温下, 添加这种水杨酸 Schiff 碱化合物对 AZ91 镁合金的腐蚀抑制作用不明显, 但在高温下, 由于合金表面化学吸附了抑制剂而使其耐腐蚀性得到增强; 随着抑制剂浓度的增加, 镁合金表面吸附更多的抑制剂, 从而使抑制作用的增强。

关键词: AZ91 镁合金; 乙二醇水溶液; 腐蚀; 抑制

(Edited by Hua YANG)